Surface & Coatings Technology xxx (2012) xxx–xxx

Contents lists available at SciVerse ScienceDirect

Surface & Coatings Technology

journal homepage: www.elsevier.com/locate/surfcoat

Oxygen-stoichiometry-dependent microstructural and magnetic properties of CoPt thin films capped with ion-beam-assisted deposited TiO_x layers

Guijun Li [a], Chi Wah Leung [b], Chin Shueh [c], Yi Jing Wu [c], Ko-Wei Lin [c],*, An-Cheng Sun [d], Jen-Hwa Hsu [e], Pui To Lai [a], Philip W.T. Pong [a],*

[a] *Department of Electrical and Electronic Engineering, The University of Hong Kong, Hong Kong*
[b] *Department of Applied Physics, Hong Kong Polytechnic University, Hong Kong*
[c] *Department of Materials Science and Engineering, National Chung Hsing University, Taichung, Taiwan*
[d] *Department of Chemical Engineering and Materials Science, Yuan Ze University, Chungli, Taiwan*
[e] *Department of Physics, National Taiwan University, Taipei, Taiwan*

ARTICLE INFO

Available online xxxx

Keywords:
Magnetic thin films
CoPt
Ion-beam assisted deposition

ABSTRACT

The magnetic properties of CoPt with different percentages of oxygen in the TiO_x capping layer were investigated through annealing processes. Results have shown that after annealing, the structural phase transformation from fcc to fct CoPt occurred and was confirmed by the enhanced coercivities. In addition, the isolated CoPt grains separated by grain boundary TiO_x in the annealed CoPt/TiO_x (30% O_2/Ar) thin films exhibited the largest coercivity. The excess amount of oxygen in the TiO_x layer may react with Co and Pt to form oxides (as characterized by XPS) and result in the drop of coercivity. Thus the growth of the fct CoPt phase can be enhanced by optimizing the oxygen ratio during fabrication of the TiO_x layer and post annealing, which may find useful applications for future CoPt-based magnetic recording.

1. Introduction

Thermal stability of magnetic thin films at the nanometer scale is one of the most critical challenges for the hard disk drives to acquire a recording density over 1 Tbit/in^2. Face center tetragonal (fct) phase CoPt has magnetocrystalline anisotropy as high as 5×10^7 erg/cm^3 and has good chemical stability, which makes fct phase CoPt a promising material for hard disk recording media [1]. Fct CoPt phase can be transformed from face center cubic (fcc) phase by annealing at 600 °C, and this transformation process has been widely investigated [2–14]. It is found that a capping layer or buffer layer with different materials can change the CoPt coercivity either by surface diffusion [5,6,8,12,14,15] or through interface texture influence [16–22]. The additional layer might also lower the phase transformation temperature of CoPt. Using a thin Cu underlayer, the 50 nm thick CoPt could be fully transformed from fcc to fct phase after annealing at 500 °C for 30 min [8]. The addition layer might also diffuse into CoPt layer and break the CoPt continuous thin film into separated grains during annealing [5]. CoPt using carbon underlayer could be fully transformed from fcc to fct phase after annealing at 400 °C, with an out-of-plane coercivity as high as 2.77 kOe; the effect originates from carbon diffusion into CoPt, which breaks the continuous CoPt film into separated grains after annealing [5]. Thus the composition, morphologies, and magnetic properties of the CoPt layer would all differ according to the buffer layer used.

Recently, Yuan et al. [12] found that the coercivity of fct phase CoPt decreased to less than 100 Oe after post-annealing over 800 °C. They explained it as a result of the large biaxial tensile stress in the CoPt thin film after annealing, which would transform the fct phase CoPt to the fcc phase [12]. Thus if the tensile stress in CoPt thin film can be removed, the coercivity of CoPt will be higher.

TiO_x has been used in magnetic recording media, such as the CoPt–TiO_2 composite perpendicular recording media. Coercivity as high as 6.7 kOe was acquired in CoCrPt–SiO_2/CoPt–TiO_2 stacked media using 16 nm thick CoPt–TiO_2 [23]. An average grain size of 5.5 nm with standard deviation of 1.1 nm was acquired using Ru_1 (10 nm)/Ru_2 (10 nm)/CoPt–TiO_2 structure [24,25]. Different oxygen stoichiometries in TiO_x might also influence the CoPt magnetic properties either via interface texturing or surface diffusion; however no such research has been reported yet.

In this paper, we report the study of CoPt/TiO_x bilayer structure with different oxygen contents, which was controlled by the O_2/Ar ratio during the ion beam bombardment process when the TiO_x layer was deposited by ion-beam-assisted deposition (IBAD). The XRD patterns, microstructures, and magnetic properties of the bilayers with different oxygen contents were examined.

---

* Corresponding authors.
E-mail addresses: kwlin@dragon.nchu.edu.tw (K-W. Lin), ppong@eee.hku.hk (P.WT. Pong).

0257-8972/$ – see front matter © 2012 Elsevier B.V. All rights reserved.
doi:10.1016/j.surfcoat.2012.05.103

Please cite this article as: G. Li, et al., Surf. Coat. Technol. (2012), doi:10.1016/j.surfcoat.2012.05.103

2. Experiment

Silicon substrates with (100) orientation were thermally oxidized at 900 °Cto form a 180 nm thick SiO_2 layer. The oxidized silicon substrates were then cleaned in acetone and ethanol with sonication. Co and Pt were co-sputtered in an Ar environment with dc power of 60 W and 34 W respectively. The base pressure was 8×10^{-9} Torr and the Ar pressure was 10 mTorr during deposition. A Kaufmann source was used to focus the Ar ion beam onto a commercial Ti target surface, while an End-Hall source was used to bombard the substrate in situ during the deposition of the TiO_x layer. The O_2 flux in the End-Hall ion source ranged from 0 to 1.6 sccm so the flow rate ratio of oxygen to argon was varied from 0% to 41%. The samples were then annealed at 600 °C for 20 min. The crystalline structures of the CoPt/TiO_x thin films were investigated by grazing angle X-ray diffraction with a Cu K_α source. A JEOL JEM-2010 transmission electron microscopy (TEM) system operating at 200 kV was used for the structural and microstructural analysis. X-ray photoelectron spectroscopy (XPS) was used to study the oxidation state and depth profile analysis using a ULVAC-PHI-5000 with Al K_α radiation. The ferromagnetic properties of the CoPt/TiO_x thin films were measured with a Lake Shore—7407 vibrating sample magnetometer (VSM).

3. Results and discussion

Our previous work in CoPt thin films [26] has shown the impact of the ion-beam bombardment on magnetic properties by directly bombarding the Co and Pt atoms during fabrication processes. In this work, we study how the capped TiO_x layer (fabricated by ion-beam assisted deposition [27]) affects the magnetic properties of CoPt/TiO_x thin films via annealing. The CoPt/Ti (i.e., 0% O_2/Ar) bilayer exhibited fct CoPt phase with a lattice constant of a = 3.70 Å, c = 3.82 Å after annealing at 600 °C for 20 min, as indexed by (001), (111), (002), (202), (311), and (113) orientations of CoPt in the XRD spectra in Fig. 1(a). The appearance of the (001) peak at 24° and (002) peak at 48° also indicates the existence of the fct CoPt phase. However, increasing the oxygen ratio during the ion bombardment of TiO_x to 21% O_2/Ar (Fig. 1(b)) or 41%O_2/Ar (Fig. 1(c)) does not change (expand or contract) the structures, as evidenced by the same CoPt lattice constants. This indicates the role of TiO_x that is used to form the grain boundary to separate CoPt grains, as characterized by TEM in the next paragraph.

High-resolution TEM (HRTEM) was used to characterize the sample structures, microstructures, surface morphologies and the bilayer interfaces, as shown in Fig. 2. The annealed CoPt/TiO_x (21% O_2/Ar) bilayers exhibited polycrystalline structures, as revealed by the TEM bright field (BF) image and electron diffraction patterns (DP) in Fig. 2 (a). The dark field (DF) image (the middle panel in Fig. 2(a)) provides the grain size distribution (Fig. 2(d)) ranging from 5 to 35 nm. Meanwhile, the annealed CoPt/TiO_x (30% O_2/Ar) bilayer has a narrower grain size distribution (ranging from 8 to 22 nm) with CoPt grains separated by grain boundary TiO_x (Fig. 2(b)), compared to those of CoPt/TiO_x (21% O_2/Ar (Fig. 2(a)) and 41% O_2/Ar (Fig. 2(c)), grain size distribution ranging from 12 to 35 nm). The representative cross-sectional TEM images of the as-deposited and annealed CoPt/TiO_x (21% O_2/Ar) thin film are shown in Fig. 2(e) and (f), respectively. The slightly reduced TiO_x thickness and rougher interface (Fig. 2(e)) indicate the oxide diffusion into the CoPt layer after annealing. The structural characterization by TEM is consistent with those obtained by XRD in Fig. 1. The different morphology due to different amount of oxygen in the TiO_x layer incorporated into the CoPt layer via annealing strongly influences the corresponding magnetic properties (see below).

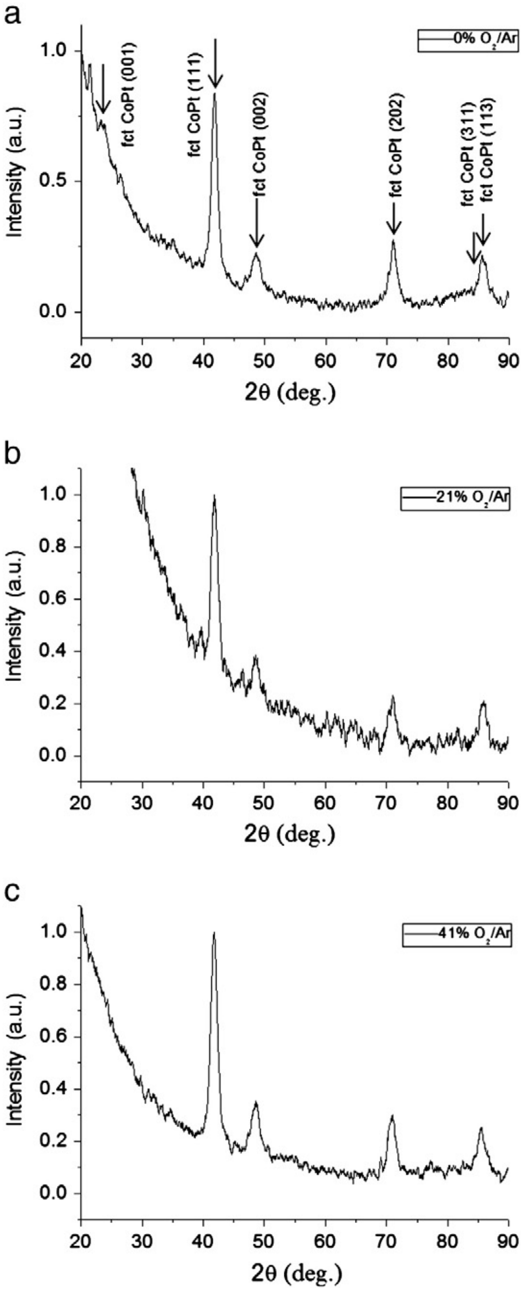

Fig. 1. XRD spectra of annealed CoPt/TiO_x thin films (600 °C, 20 min) with different oxygen ratios. (a) Pure CoPt (i.e., 0% O2/Ar), (b) CoPt/TiO_x (21% O_2/Ar), and (c) CoPt/TiO_x (41% O_2/Ar).

To further probe the annealing effects on the distribution of elements (such as Co, Pt, and O) at the interface between TiO (top), CoPt (middle), and SiO_2 (bottom) layers, X-ray Photoelectron Spectroscopy (XPS) [28] analysis was performed in terms of binding energies and depth profile [29], as shown in Fig. 3. First, in the top TiO_x layer, the Titanium exhibited both metallic (Ti^{0+} (~454 eV)) and complex oxidation states (Ti^{3+} (~456 eV) and Ti^{4+} (~458 eV)), as confirmed by the fitted results by Shirley procedure [30] shown in Fig. 3(a). The presence of oxygen is evidenced by the peak of O1s spectrum at ~529 eV, as shown in Fig. 3(b). Second, in the middle CoPt layer, the observed binding energies of Co and Pt indicate that the oxidation processes (CoO and PtO) that occur due to the annealing processes, as shown by the peak positions at ~781 eV (CoO) and at ~73 eV (PtO), in addition to the metallic Co (~777 eV) and Pt (~70 eV) phases. Third, in the bottom SiO_2 layer, the substrate signal from Si is shown by the peak at ~104 eV in Fig. 3(e). After identifying the bonding types and/or oxidation states in the annealed CoPt/TiO_x thin films, the diffusion behavior due to annealing is further revealed by the depth profile analysis by XPS in Fig. 3(f). In the top TiO_x layer (marked by region I), the Co

Please cite this article as: G. Li, et al., Surf. Coat. Technol. (2012), doi:10.1016/j.surfcoat.2012.05.103

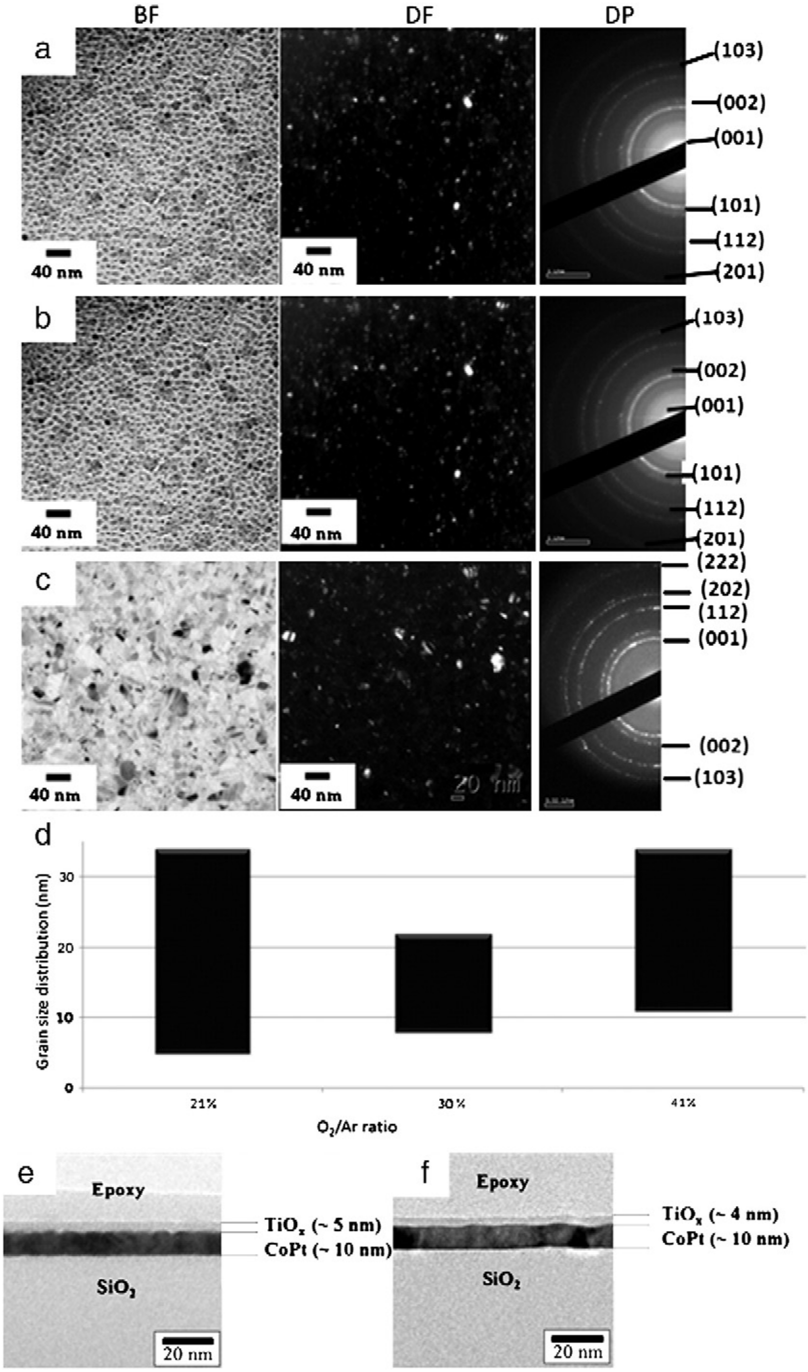

Fig. 2. TEM images of annealed CoPt/TiO$_x$ thin films with (a) 21% O$_2$/Ar, (b) 30% O$_2$/Ar, and (c) 41% O$_2$/Ar. Each set consists of bright-field (BF) image, dark-field (DF) image, and diffraction patterns (DP). The relation between grain sizes and oxygen-stoichiometry is shown in (d). The representative cross-sectional TEM images of the as-deposited and annealed CoPt/TiO$_x$ (21% O$_2$/Ar) thin film are shown in (e) and (f), respectively.

and Pt signals increase with sputter time indicating diffusion processes of Co and Pt in the middle CoPt layer (region II) due to annealing [31–33]. In contrast, the oxygen signal drops quickly near the boundary between region I and II, which indicates that oxygen distribution is not uniformly distributed throughout the CoPt layer until about half the region II (sputter time ~0.6 min) where onset of oxygen concentration is observed. In addition, the Si diffusion from region III to II is found by the Si signal near the interface between CoPt and SiO$_2$. Therefore, the XPS analysis of the annealed CoPt/TiO$_x$ (30% O$_2$/Ar) thin film provides the important information in (1) the bonding types of elements such as Co, Pt, and Ti, and (2) the distribution of the respective elements due to annealing. These results are consistent with those characterized by XRD and TEM.

In order to investigate the relation between magnetic properties of CoPt/TiO$_x$ bilayers and oxygen contents, in-plane hysteresis loops were measured at room temperatures (Fig. 4). The as-deposited CoPt/TiO$_x$ (0% O$_2$/Ar) thin film exhibited soft magnetic properties with coercivity, Hc ~48 Oe, as shown in Fig. 4(a). Similar soft magnetic properties (coercivities about 50 Oe) and hysteresis loop shapes were observed in CoPt/TiO$_x$ thin films with different percentages of oxygen (21, 30 and 41% O$_2$/Ar) in the top TiO$_x$ layer. This is consistent with the fact that the measured signals are contributed from the

Please cite this article as: G. Li, et al., Surf. Coat. Technol. (2012), doi:10.1016/j.surfcoat.2012.05.103

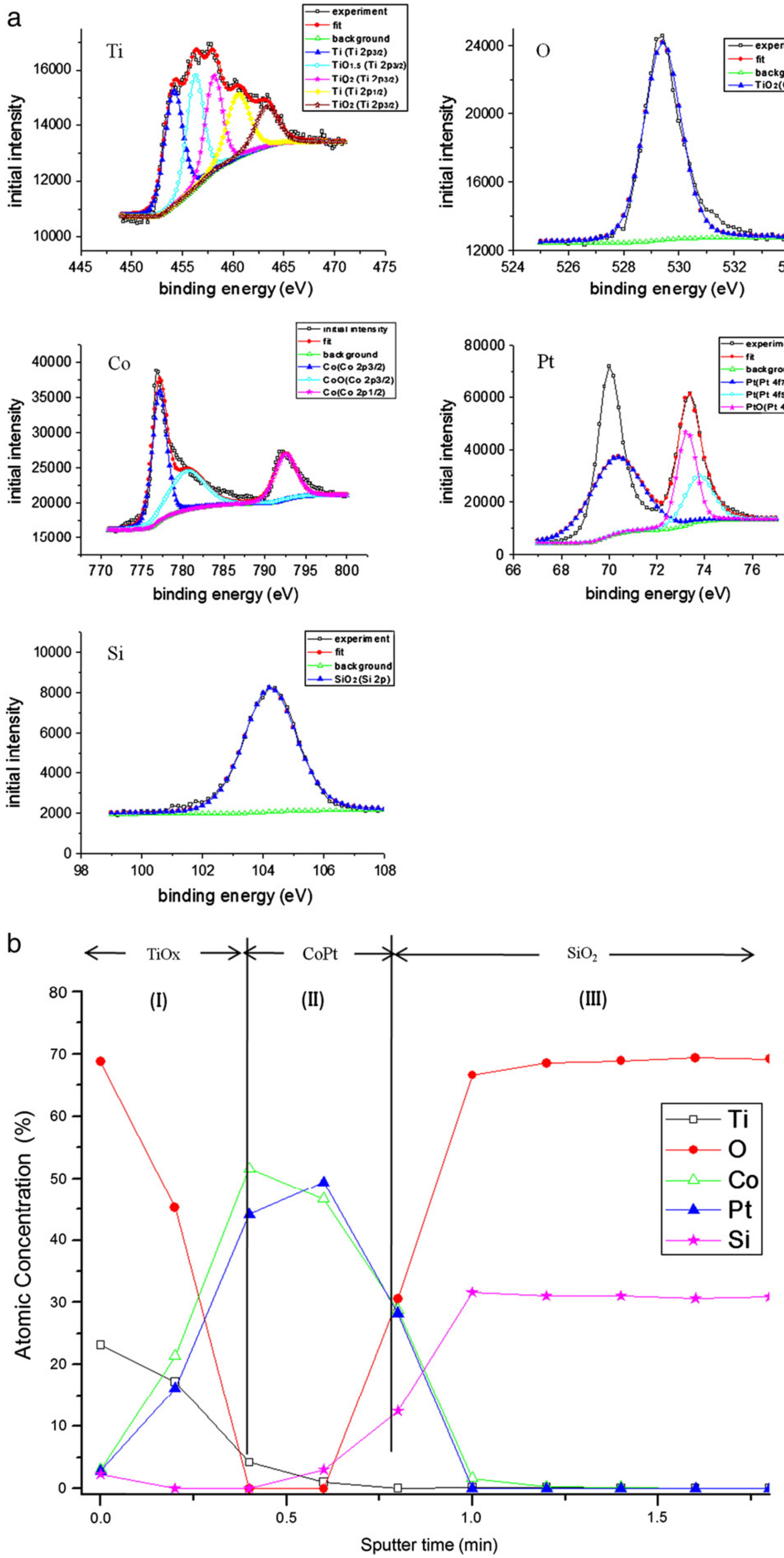

Fig. 3. XPS analysis in the annealed CoPt/TiO_x (30% O_2/Ar) thin film for (a) the binding energies in Ti, O, Co, Pt, and Si; and (b) the depth profile.

ferromagnetic bottom CoPt layer. However, the enhanced coercivity dependence of %O_2/Ar was observed in the annealed CoPt/TiO_x thin films, as shown in Fig. 4(b). For these annealed CoPt/TiO_x thin films, the coercivity increases with increasing O_2/Ar from Hc ~200 Oe (CoPt/TiO_x (0% O_2/Ar)) to the largest Hc ~405 Oe (CoPt/TiO_x (30% O_2/Ar)), as shown in Fig. 4(c). Further increasing the %O_2/Ar to 41% O_2/Ar results in a drop in Hc (~340 Oe). First, the enhanced coercivities of the annealed CoPt/TiO_x thin films are attributed to the formation of fct CoPt structures due to the annealing processes (compared to those of the as-deposited CoPt/TiO_x thin films), as confirmed by the structural and microstructural characterization by XRD and TEM. Second, the increased Hc with increasing %O_2/Ar in the annealed CoPt/TiO_x thin films may result from excess oxygen atoms serving pinning sites to hinder the magnetization reversal process. The formation of CoO or PtO by consuming fct CoPt may give rise to the drop in Hc in an annealed CoPt/TiO_x with the highest %O_2/Ar (41% O_2/Ar), as evidenced by the XPS analysis.

Based on the characterization results by XRD in structures, by TEM in structures and microstructures, by XPS in elemental bonding types, oxidation states, and depth profile, and by VSM in magnetic properties, we concluded that (1) the phase transformation from fcc to fct CoPt gives rise to the enhanced coercivities, (2) the oxygen distribution depends on different amount of oxygen in the TiO_x layer through annealing processes, and (3) the magnetic properties of the annealed CoPt/TiO_x thin films are strongly influenced by the oxygen-stoichiometry incorporated with Ti atoms through ion-beam-assisted deposition processes.

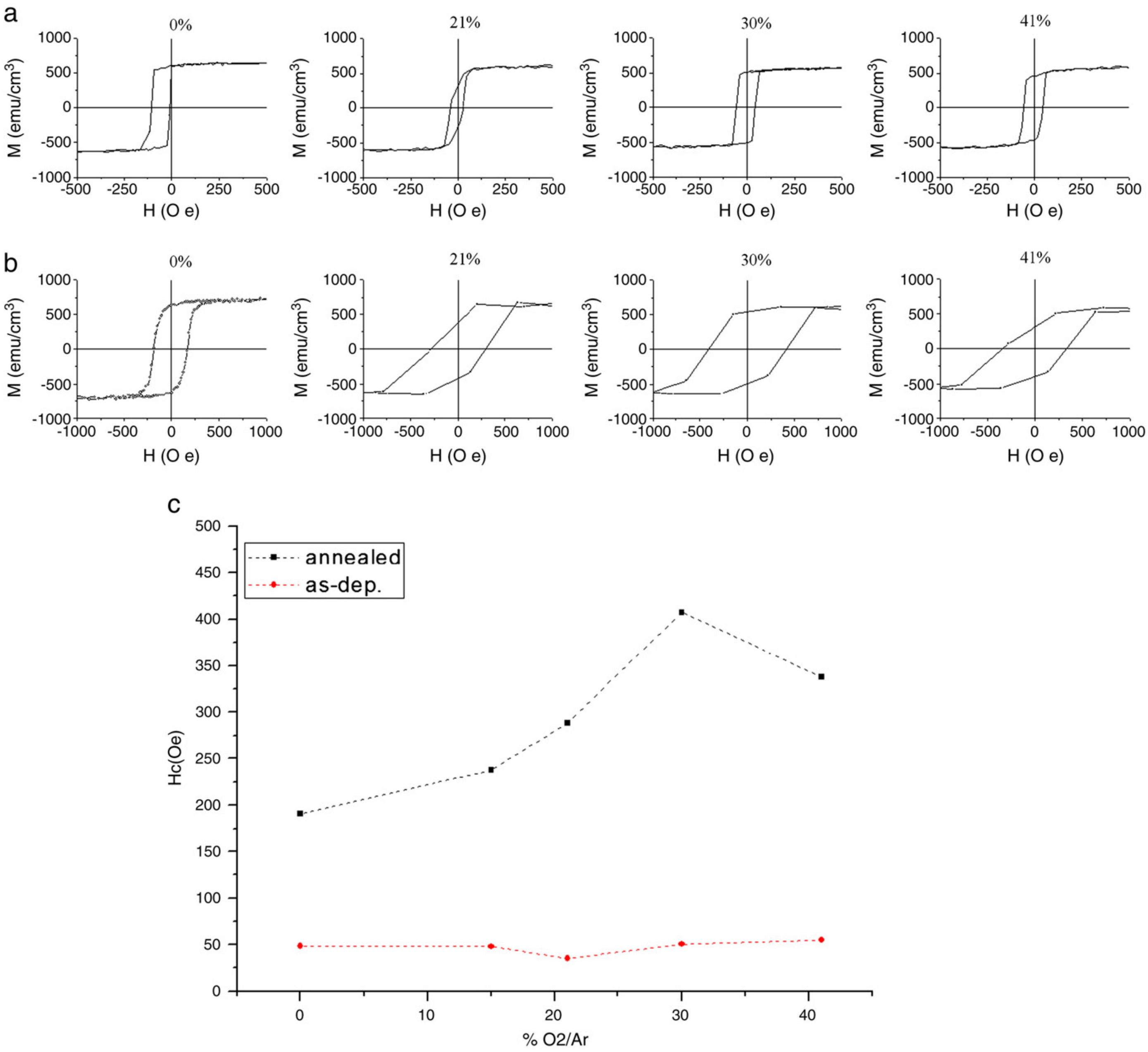

Fig. 4. The in-plane hysteresis loops of (a) as-deposited and (b) annealed CoPt/TiO_x (0–41% O_2/Ar) thin films. The coercivity dependence of oxygen ratios in annealed CoPt/TiO_x thin films is shown in (c).

Please cite this article as: G. Li, et al., Surf. Coat. Technol. (2012), doi:10.1016/j.surfcoat.2012.05.103

4. Conclusion

The structural, microstructural, and magnetic properties of annealed CoPt/TiO_x thin films were studied. While the enhanced coercivities of annealed CoPt/TiO_x thin films are attributed to the structural phase transformation from fcc to fct CoPt, different amount of oxygen in TiO_x layers can be used to modify the distribution of oxygen atoms and thus give rise to either the enhanced Hc (thus CoPt ordering) or drop in Hc (formation of CoO or PtO compound with excess oxygen atoms).

Acknowledgment

This work was supported by the Seed Funding Program for Basic Research from the University of Hong Kong, the RGC-GRF grant (HKU 7049/11P), the RGC-GRF grant (PolyU 5013/08P), the Ministry of Economic Affairs of Taiwan and National Science Council of Taiwan.

References

[1] P. Brissonneau, A. Blanchard, H. Bartholin, IEEE Trans. Magn. 2 (1966) 479.
[2] C.W. White, S.P. Withrow, J.D. Budai, D.K. Thomas, J.M. Williams, A. Meldrum, K.D. Sorge, J.R. Thompson, G.W. Ownby, J.F. Wendelken, L.A. Boatner, J. Appl. Phys. 98 (2005) 114311.
[3] T. Allmers, M. Donath, Phys. Rev. B 81 (2010) 064405.
[4] B. An, L. Zhang, S. Fukuyama, K. Yokogawa, Phys Rev B 79 (2009) 085406.
[5] J. Du, S. Wang, C. Ruby, A. Khapikov, W.J. Liu, J.A. Barnard, J.W. Harrell, J. Magn. Magn. Mater. 231 (2001) 231.
[6] J. Kim, K. Barmak, M. De Graef, L.H. Lewis, D.C. Crew, J. Appl. Phys. 87 (2000) 6140.
[7] M.T. Lin, J. Shen, W. Kuch, H. Jenniches, M. Klaua, C.M. Schneider, J. Kirschner, Phys Rev B 55 (1997) 5886.
[8] E. Manios, V. Alexandrakis, D. Niarchos, J. Magn. Magn. Mater. 316 (2007) E166.
[9] S. Shiomi, T. Nakakita, T. Kobayashi, M. Masuda, Jpn. J. Appl. Phys. Part 2 Lett. 32 (1993) L1058.
[10] F.J. Yang, H. Wang, H.B. Wang, J. Zhang, J.H. Zhu, Q. Li, Y. Jiang, J. Phys. D Appl. Phys. 42 (2009) 115001.
[11] F.T. Yuan, H.W. Chang, W.M. Liao, S.N. Hsiao, S.K. Chen, Y.D. Yao, H.Y. Lee, J. Appl. Phys. 101 (2007) 09K526.
[12] F.T. Yuan, H.W. Huang, W.M. Liao, H.W. Chang, A.C. Sun, S.N. Hsiao, S.K. Chen, H.Y. Lee, IEEE Trans. Magn. 45 (2009) 2682.
[13] A. Markou, I. Panagiotopoulos, T. Bakas, J. Magn. Magn. Mater. 322 (2010) L61.
[14] R.J. Tang, W.L. Zhang, Y.R. Li, J. Magn. Magn. Mater. 322 (2010) 3490.
[15] X.H. Xu, T. Jin, X.L. Li, F. Wang, F.X. Jiang, H.S. Wu, Thin Solid Films 515 (2007) 3936.
[16] J.N. Zhou, D. Otte, J.A. Barnard, IEEE Trans. Magn. 36 (2000) 2683.
[17] P. Kappenberger, S. Martin, Y. Pellmont, H.J. Hug, J.B. Kortright, O. Hellwig, E.E. Fullerton, Phys. Rev. Lett. 91 (2003) 267202.
[18] V.G. Kravets, L.V. Poperenko, I.V. Yurgelevych, D.Y. Manko, J. Magn. Magn. Mater. 290 (2005) 562.
[19] T. Hiratsuka, G. Kim, Y. Sakuraba, T. Kubota, K. Kodama, N. Inami, H. Naganuma, M. Oogane, T. Nakamura, K. Takanashi, Y. Ando, J. Appl. Phys. 107 (2010) 09C714.
[20] B. Kagerer, C. Binek, W. Kleemann, J. Magn. Magn. Mater. 217 (2000) 139.
[21] D.C. Crew, J. Kim, L.H. Lewis, K. Barmak, J. Magn. Magn. Mater. 233 (2001) 257.
[22] K.K.M. Pandey, J.S. Chen, G.M. Chow, B.C. Lim, J. Magn. Magn. Mater. 321 (2009) 3236.
[23] S.H. Park, T.D. Lee, S.H. Kong, S.Y. Yoon, H.S. Lee, H.J. Kim, H.S. Oh, J. Appl. Phys. 103 (2008) 07F528.
[24] M.W. Song, S.H. Park, W.B. Byun, S.O. Kim, T.D. Lee, IEEE Trans. Magn. 45 (2009) 2690.
[25] G.J. Li, C.W. Leung, Z.Q. Lei, K.W. Lin, P.T. Lai, P.W.T. Pong, Thin Solid Films 519 (2011) 8307.
[26] K.W. Lin, J.Y. Guo, S.R. Lin, H. Ouyang, C.J. Tsai, J. van Lierop, N.N. Phuoc, T. Suzuki, Phys. Status Solidi C 4 (2007) 4507.
[27] K.W. Lin, M. Mirza, C. Shueh, H.R. Huang, H.F. Hsu, J. van Lierop, Appl. Phys. Lett. 100 (2012) 122409.
[28] K.W. Lin, F.T. Lin, Y.M. Tzeng, IEEE Trans. Magn. 41 (2005) 927.
[29] B.O. Olanrewaju, J. Herring-Captain, G.A. Grieves, A. Aleksandrov, T.M. Orlando, J. Phys. Chem. A 115 (2011) 5936.
[30] D.A. Shirley, Phys. Rev. B 5 (1972) 4709.
[31] H. Yoshida, N. Sato, Chem. Phys. Lett. 511 (2011) 146.
[32] P.J. Cumpson, J. Electron. Spectrosc. 73 (1995) 25.
[33] Y.-J. Chen, C.-C. Chang, H.-Y. Ho, J.-S. Tsay, Thin Solid Films 519 (2011) 8343.